Sensors & Actuators: B. Chemical 290 (2019) 640–647

Contents lists available at ScienceDirect

Sensors and Actuators B: Chemical

journal homepage: www.elsevier.com/locate/snb

Fluorometric and colorimetric analysis of carbamate pesticide via enzyme-triggered decomposition of Gold nanoclusters-anchored MnO_2 nanocomposite

Xu Yan[a,*], Deshuai Kong[a], Rui Jin[a], Xu Zhao[a], Hongxia Li[a], Fangmeng Liu[a], Yuehe Lin[b], Geyu Lu[a,**]

[a] State Key Laboratory on Integrated Optoelectronics, College of Electronic Science and Engineering, Jilin University, 2699 Qianjin Street, Changchun, 130012, China
[b] School of Mechanical and Materials Engineering, Washington State University, Pullman, WA 99164, United States

ARTICLE INFO

Keywords:
AuNCs-MnO_2 composite
Carbamate pesticide
Enzyme
Dual-readout

ABSTRACT

In this work, we designed a multi-signal readout platform for sensitive monitoring carbamate pesticide based on gold nanoclusters-anchored MnO_2 (AuNCs-MnO_2) nanocomposite. The fluorescence of AuNCs was quenched by MnO_2 via Förster resonance energy transfer effect. In the presence of acetylcholinesterase and choline oxidase, the substrate acetylcholine (ACh) is catalyzed to generate H_2O_2 that can specially induce the decomposition of MnO_2, coupling with change of color and recovery of fluorescence. Carbamate pesticide as an inhibitor of acetylcholinesterase prevent the generation of H_2O_2, further block the breakage of MnO_2, which caused the fluorescence switch. Such color and fluorescence respond can be utilized for highly sensitive carbamate pesticide identification and quantification. Under the optimum conditions, the dual-output assay possessed good sensitivity for rapid detection of carbaryl (model analyte) with a detection limit of 0.125 μg L^{-1}. The fluorometric/colorimetric bimodal platform showed good stability and anti-interference ability comparing to that of others enzyme-based sensor.

1. Introduction

Carbamate pesticide are extensively used in modern agriculture to boost crop yield, due to their high lethality towards insects [1]. Unfortunately, the residue of carbamate pesticide not only seriously destroy the ecosystem, but also obviously trigger food contamination. More importantly, on the base of bioaccumulation effects in human body [2,3], carbamate pesticide can effectively suppress the activity of acetylcholinesterase (AChE) that plays curial roles in central and peripheral nervous system [4–6], possessing persistent damage to public health. To monitoring and prevent pesticide contamination, facile and accurate detection of carbamate pesticide residues in food has become urgent demand for the protection of consumer health [7].

Fluorescence-based strategy has considered to be a promising approach that can be applied for sensitive and selective detection of carbamate pesticide, due to its efficiency, cost-saving, and easy-operation [8–11]. Among these, AChE-based fluorometric sensing assay have been exploited extensively for detecting pesticide [12–15]. In the case of AChE-based platforms, pesticide possess the ability of irreversible inhibition of enzyme, which suppress the activity to catalytically hydrolyze acetylthiocholine (ATCh) or acetylcholine (ACh), further inducing the responds of system signal [16]. Using the above process, rhodamine B-covered gold nanoparticles (RB-AuNPs) were employed as signal indicator to recognize enzymatic product (thiocholine), indirectly responding to pesticide [17]. Inspired by this work, thiocholine with the chemically reactive group (-SH) that can react with metal cations [18,19], silver nanoparticles [20,21] and AuNPs [22,23], act as an analyte-marker for pesticide monitoring. However, the unstable thiocholine can be oxidized during the sensing process. Furthermore, those strategies were easily influenced by co-existing chemicals including other thiol-containing compounds, cyanide, salt, and protein, due to the interaction between chemicals and silver/gold nanoparticles [24]. To overcome these drawbacks, bi-enzyme platforms with acceptable stability and sensitivity have been utilized for pesticide detection. In general, bi-enzyme system is composed of AChE and choline oxidase (ChOx), in which catalyze ACh to produce hydrogen peroxide (H_2O_2). H_2O_2 as a “bridge” can link the bi-enzyme format and optical probe, which can be used for indirectly fabricating pesticide sensor. On the

* Corresponding author.
** Corresponding author.
E-mail addresses: yanx@jlu.edu.cn (X. Yan), lugy@jlu.edu.cn (G. Lu).

https://doi.org/10.1016/j.snb.2019.04.045
Received 26 February 2019; Accepted 8 April 2019
Available online 09 April 2019
0925-4005/

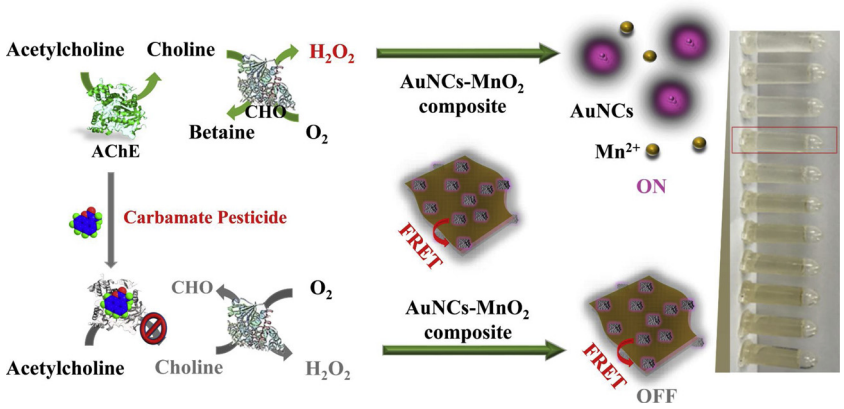

Scheme 1. Schematic illustration of the dual-signal system for carbamate pesticide detection.

basis of bi-enzyme format, fluorescent dye [25], quantum dots [26,27], silicon dots [28] and carbon dots [29] were served as H_2O_2-recognizer to fabricate platform for quantitative analysis of pesticide. Although these systems exist good selectivity for pesticide detection, most of bi-enzyme platforms were suffered from low sensitivity and background interference. For application in complex systems, the background signal is also subjected to the influence of the sample matrix, which would induce false-negative results. Hence, we aim to fabricate a bi-enzyme platform which can improve the performance of biosensor for pesticide detection and avoid the interference from co-existing chemicals.

Enlightened by the above-mentioned development, by combining the specificity of bi-enzyme and the nanomaterials-assisted target recognition, we design a novel fluorometric/colorimetric bimodal sensor for the highly accurate detection pesticide. As shown in Scheme 1, we synthesized gold nanoclusters-anchored manganese dioxide (AuNCs-MnO_2) nanocomposite with excellent stability by exploiting bovine serum albumin (BSA) as a “co-template”. Considering that the MnO_2-induced FL quenching effect can be reversed via introducing the bi-enzyme of AChE and CHO [30], AuNCs-MnO_2 composite was used to sensing bi-enzyme reaction process. Carbaryl as the model carbamate pesticide can efficiently inhibit the activity of AChE, further suppress the decomposition of MnO_2, accompanying the obvious FL quenching again and absorbance change. By recording the spectral output signal switch, the AuNCs-MnO_2/AChE/CHO system is successfully applied to colorimetrically and fluorometrically detect pesticide with good performance on selectivity, and sensitivity. In this proposed platform, AuNCs-MnO_2 composite with good stability can conquer the drawback of poor monodispersity of fluorophore-MnO_2 nanocomposites [24,31,32]. Meanwhile, the specific recognition of AChE and CHO, the excellent inhibition ability of carbaryl, and the pre-processing procedure of samples can inhibit the negative effect of reducing agents [31,33–35], thiol-containing compounds and other co-existing substance, improving the specificity of nanoplatform. Furthermore, the fluorometric/colorimetric bimodal output can improve the accuracy and reliability based on the self-verification of results [36,37]. The integration of the merits in this nanoplatform provides outstanding potentials for sensitive detection of carbaryl remained from agricultural and food sample.

2. Results and discussion

2.1. Controllable synthesis and characterization of AuCNs-MnO_2 composite

The BSA-stabilized synthesis of AuCNs-MnO_2 composite was prepared by a co-template hydrothermal reaction [38] (Fig. 1A). Firstly, AuNCs were prepared by protein-directed biomimetic synthesis method [39]. The morphology of as-synthesized AuNCs were measured with the homogeneous size around 3.3 ± 0.7 nm by transmission electron microscopy (TEM) as shown in Fig. S1 A. Specifically, the AuNCs possess excellent red emission (red line) at 370 nm excitation and strong absorbance (black line, Fig. S1B). Then the as-prepared AuNCs were mixed with Mn^{2+} under vigorous stirring, where BSA can seize Mn^{2+} through the coordination facility of amide groups and thiol groups in the protein backbone. These AuNCs-Mn^{2+} complexes provide a location for nucleation of the crystals. Under alkaline solution (Figs. S2 and S3), Mn^{2+} was spontaneously oxidized into MnO_2 crystals with the help of dissolved oxygen. The nanocomposite not only displayed the typical MnO_2 characters with broad absorption spectrum in the range from 300 to 550 nm, originating from the d–d transition of Mn ions in the MnO_6 octahedra, but also showed the FL spectra as emission position with AuNCs at 620 nm.

To further confirm the formation of AuNCs-MnO_2 nanocomposite, various microscopic and spectroscopic methods were used to characterize the morphology and structure of nanocomposite. The transmission electron microscope (TEM) result illustrated that the AuNCs-MnO_2 composites were 2D morphology with lateral dimension of about 60 nm (Fig. 1B). The hydrodynamic diameter of AuNCs-MnO_2 composites collected by dynamic light scattering (DLS) were 71.1 nm. High-magnification TEM images (Fig. 1C) revealed that AuNCs with lattice spacing of 0.238 nm are successfully interspersed on the surface of MnO_2 nanosheets (NSs) whose lattice fringe were 0.212 nm. The typical scanning electron microscopy (SEM) image illustrated the sheet-like structure of MnO_2 NSs whose surface loaded numerous of AuNCs (Fig. S4). The mapping image were also confirmed the presence of Mn and Au in nanocomposite (Fig. S5). The phase structures of the nanocomposites were characterized by X-ray powder diffraction (XRD). As shown in Fig. 1D, the diffraction peaks at 25.2°, 38.5° and 63.2° (2θ) from the AuNCs-MnO_2 were in good agreement with the standard XRD pattern of MnO_2 crystal phase (JCPDS 43–1455). And peak at 40° and 46.5° can also be indexed as Au (111) and Au (220) planes that were aligned with the bulk Au crystal phase. Thus, the aforementioned characterizations proved the successful synthesis of AuNCs-MnO_2 composites. Compared with the conventional methods for the fabrication of hybrid system through postassembly process, the developed “co-template” strategy highly simplified the operation procedure via integration of the nanomaterial synthesis. In addition, the photostability and chemical stability of nanocomposite are key characteristic for practical applications of AuNCs-MnO_2 composite. The FL emission of the nanocomposite was measured in time-course form under the continuous excitation at 370 nm (Fig. S6A). The photobleaching curves indicated that AuNCs-MnO_2 composite possess good photostability within 3600 s. As displayed in Fig. S6B, the normalized intensity of AuNCs-MnO_2 composite kept almost invariable when pH value change from 6.5–10.0. Subsequently, the FL intensity of composite showed little change in a wide Na^+ strength (0–50 mmol L^{-1}), indicating that AuNCs-MnO_2 composite shows high tolerance to salt solution (Fig.

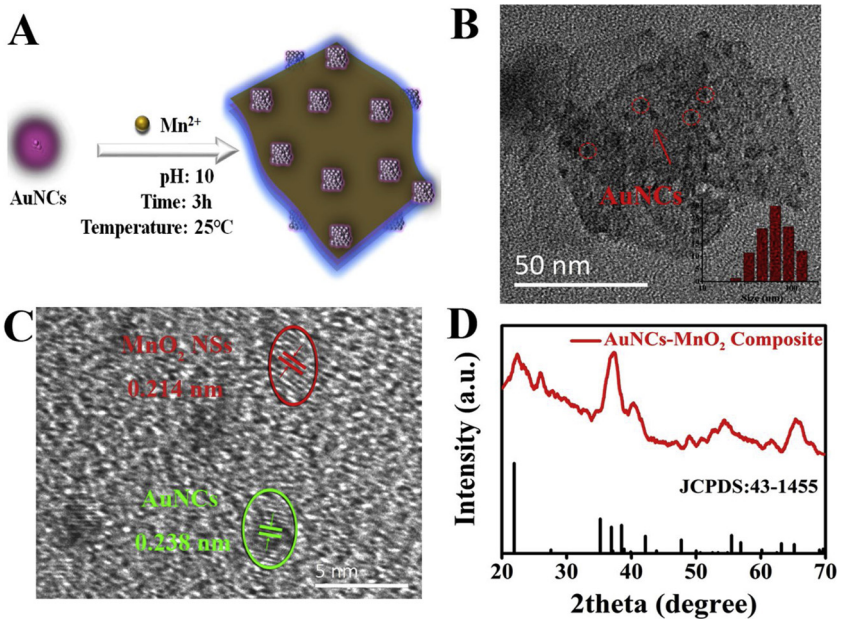

Fig. 1. (A) Co-template synthesis for AuNCs-MnO_2. (B) TEM image of AuNCs-MnO_2 and corresponding mapping image. (C) High-magnification TEM image of AuNCs-MnO_2. (D) XRD pattern of AuNCs-MnO_2.

S6C). Finally, we also surveyed that the nanocomposite still had stable FL intensity even preserved for more than 6 days at room temperature (Fig. S6D), demonstrating that the AuNCs-MnO_2 composite possess good stability at room temperature. All above results indicated that the acceptable FL behavior and outstanding stability make AuNCs-MnO_2 composite be an ideal candidate for analytical application.

2.2. Design of sensing platform

Taking their excellent optical characteristic into account, AuNCs-MnO_2 composite can be applied to pesticide-responsive analysis. In this sensing platform, AChE catalyze acetylcholine chloride (ACh) to produce choline (1). Then, the product is in turn catalytically oxidized by CHO to yield betaine and H_2O_2 (2).

$$\text{Acetycholine chloride} + H_2O \xrightarrow{\text{Acetycholinesterase}} \text{Choline} + \text{Acetic acid} \quad (1)$$

$$\text{Choline} + O_2 \xrightarrow{\text{Choline oxidase}} \text{Beatain} + H_2O_2 \quad (2)$$

H_2O_2 can obviously destroy MnO_2 NSs to form Mn^{2+} (3), establishing an "turn-on" format for sensing the inhibitor of AChE that can mediate enzymatic assay of ACh to produce H_2O_2 (Fig. S7A). As shown in Fig. 2A, the separately substance (AChE, CHO and ACh) cannot influence the FL signal, whereas the bi-enzyme of AChE/CHO-mediated reaction of ACh to produce H_2O_2 can efficiently reversed the quenched FL intensity at 638 nm of AuNCs-MnO_2 composite. The reduction product (Mn^{2+}) was confirmed by a specifically chemical redox reaction with IO_4^- (4).

$$MnO_2 + H_2O_2 + 2H^+ \rightarrow Mn^{2+} + 2H_2O + O_2 \quad (3)$$

$$2Mn^{2+} + 5IO_4^- + 3H_2O \rightarrow 2MnO_4^- + 5IO_3^- + 6H^+ \quad (4)$$

After oxidized by IO_4^-, the UV–vis absorption spectra of solution were matched well with that of MnO_4^- from 450 to 600 nm (Fig. 2B and 2C), clearly indicating that the presence of Mn^{2+}. Furthermore, the response of AuNCs to H_2O_2 and Mn^{2+} was negligible within 0–35 μmol L^{-1} and 0–25 mmol L^{-1}, respectively (Figs. S7B and S8), further confirming the feasibility of strategy. Importantly, the increase of FL intensity can be reversed by introducing carbaryl that could efficiently inhibit the activity of AChE (Fig. 2A), implying that the established sensor was appropriate for monitoring carbamate pesticides.

As shown in Fig. 2D, the FL of system exhibited remarkably gradient quenching with the increasing Mn^{2+} concentration (from 0 to 200 μmol L^{-1}), because more and more MnO_2 NSs generated (Fig. 2E). To investigate the quenching mechanism, the ζ-potential measurement and FL lifetime was measured. As revealed in Fig. 2F, the zeta potential of MnO_2 NSs and AuNCs were -21.3 mV and -28.2 mV, respectively, indicating that no electrostatic attraction between the MnO_2 NSs and AuNCs. While, compared with those two materials, AuNCs-MnO_2 composite possess better stability and dispersity owing to it lower value of zeta potential (-36.4 mV), which also shortened the distance between MnO_2 NSs and AuNCs. The FL lifetime of AuNCs-MnO_2 composite was further obtained in Fig. 2G, and the decay components and their ratios were also displayed in Table S1. The FL decay curve was fitted by utilizing a double-exponential function for getting an average lifetime that calculated to be 6.44 μs. Through controlling Mn^{2+} concentration to regulate the MnO_2 NSs, the lifetimes of AuNCs-MnO_2 composite were gradually shortened from 6.44 μs to 4.18 μs, suggesting that the energy transfer process serve as the dominant role in quenching mechanism. Moreover, increase of temperature boost a clear enhance of the quenching effect of MnO_2 NSs, further revealing dynamic quenching (Fig. 2H). Thus, the above results demonstrated that the Förster resonance energy transfer (FRET) effect between AuNCs and MnO_2 NSs regulated the FL intensity of composite.

2.3. Sensitive detection of carbaryl

To investigate the availability of the proposed sensor for monitoring of pesticide, the response to H_2O_2 and AChE were firstly measured. The designed platform for the detection of H_2O_2 was developed under the optimum conditions (Fig. S9). As shown in Fig. S10, the FL intensity of AuNCs-MnO_2 nanocomposite was gradually increased and the absorbance intensity of system was obviously decreased with the increase of H_2O_2 concentrations (from 0 to 30 μmol L^{-1}), indicating that the AuNCs-MnO_2 nanocomposite in response to H_2O_2 with dose-dependent. For AChE detection, the incubation temperature and reaction time and the pH condition were optimized to achieve good performance (Fig. S11). With the increasing of AChE, the FL intensity was gradually recovered at 630 nm (Fig. 3A). Fig. 3B shows the good correlation

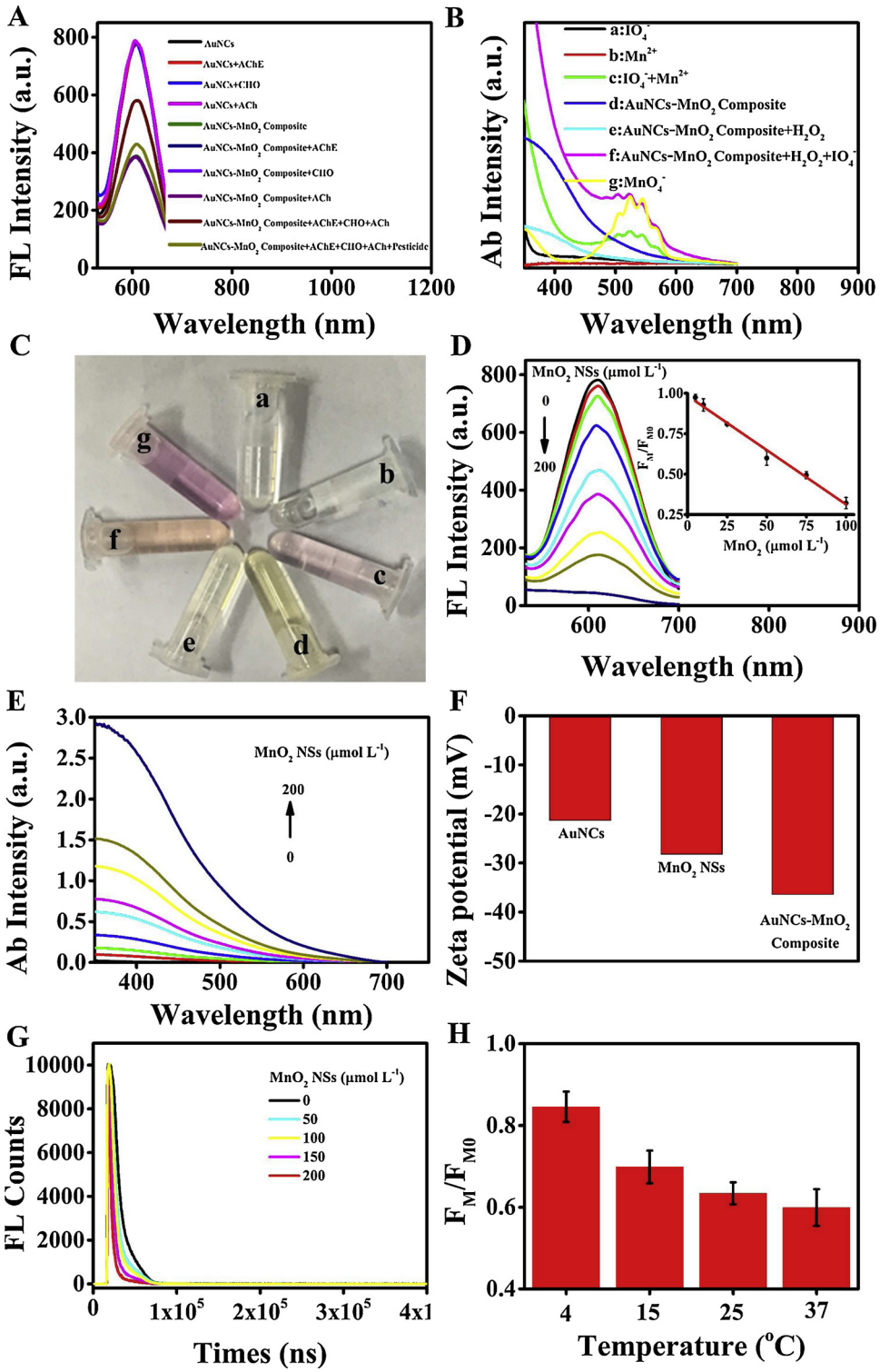

Fig. 2. (A) Feasibility of probe. (B) The UV–vis absorption spectra of IO_4^-, Mn^{2+}, $IO_4^- + Mn^{2+}$, AuNCs-MnO_2 composite, AuNCs-MnO_2 composite + H_2O_2, AuNCs-MnO_2 composite + H_2O_2 + IO_4^- and MnO_4^-. (C) Photographic image of corresponding solution. (D) FL spectra of AuNCs-MnO_2 composite in the presence of various concentrations of MnO_2 NSs. (E) Ab spectra of AuNCs-MnO_2 composite in the presence of various concentrations of MnO_2 NSs. (F) Zeta potential of AuNCs and AuNCs-MnO_2 composite. (G) Fluorescence lifetime of AuNCs-MnO_2 composite. (H) The effect of temperature.

($R^2 = 0.99$) between the F_A/F_{A0} ratio and the concentrations of AChE from 0 to 50 mU mL^{-1}. This process was further verified by UV–vis spectroscopy (Fig. 3C), accompanying that the color of reaction system was progressively faded from brown to colorless (Fig. 3D). These results demonstrated that the analysis strategy for AChE is feasible based on the "bridge" substance of H_2O_2.

Bestowed with the good performance of the AuNCs-MnO_2-AChE − CHO system, the established FRET-based assay served as an optical tracer for screening and detection of carbamate pesticide. With the aid of the inhibition property of carbaryl [29], this enzyme-triggered FL recovery can be effectively blocked by carbaryl, leading to the FL quenching of AuNCs-MnO_2 composite again. Under optimal

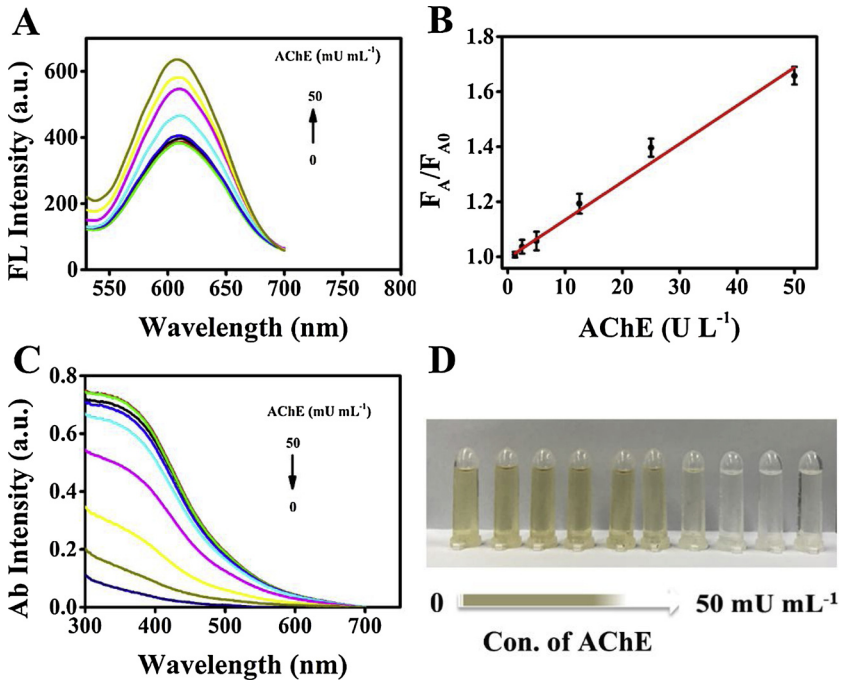

Fig. 3. (A) FL spectra of AuNCs-MnO_2 composite with various concentrations of AChE. (B) the linear range between F_A/F_{A0} and AChE. (C) UV–vis absorption spectra of sensing system in the presence of different concentration of AChE. (D) Photographic image of corresponding solution.

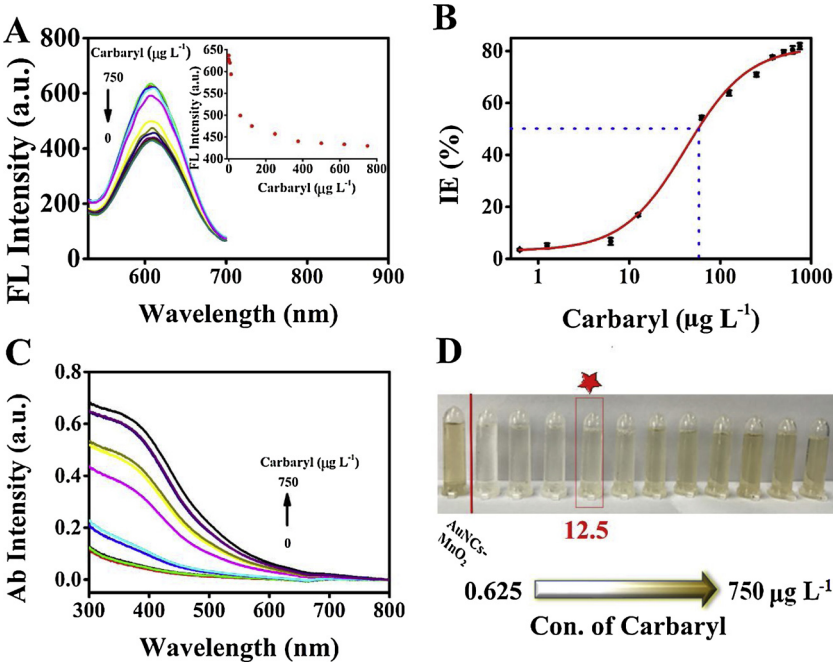

Fig. 4. (A) FL spectra of AuNCs-MnO_2 composite/AChE/CHO with various concentrations of carbaryl, inset shows the change trend of the FL intensities. The concentration of carbaryl were 0, 0.625, 1.25, 6.25, 12.5, 62.5, 125, 250, 375, 500, 625 and 750 μg L^{-1}. (B) Standard curve plot of IE (%) versus the concentration of carbaryl. (C) UV–vis absorption spectra of sensing system in the presence of different concentration of carbaryl. (D) Photographic image of corresponding solution.

conditions (Fig. S12), the FL intensity of system was gradually restored with increasing concentration of carbaryl (Fig. 4A). As revealed in Fig. 4B, values of inhibition efficiency (IE, Equation S1) were gradually growing along with carbaryl concentration increasing from 0.125–750 μg L^{-1} in the AuNCs-MnO_2-AChE − CHO system. The proposed platform showed excellent linearity (R^2 = 0.997) responses for detecting carbaryl with the average IC_{50} value (half-maximal inhibitory concentration) of 41.8 μg L^{-1}. The detection limit for carbaryl was estimated to be 0.125 μg L^{-1}, which was much lower than the value (1000 μg L^{-1}) of the maximum residue limit set by the Chinese National food safety standard (GB-2763 − 2014), indicating that the proposed sensor can meet the detection requirement. Furthermore, this process was also confirmed by UV–vis spectroscopy, that is, the characteristic absorption peak at 350 nm of MnO_2 NSs was rising up with the increase of carbaryl (Fig. 4C). Meanwhile, the reaction solution produced noticeable chromatic changes from colorless to brown (Fig. 4D), which showed a dose-responsive color change to carbaryl. More importantly, our eyes' sensitivity is good enough to distinguish the obvious color variations for the quantitative detection of carbaryl even down to 12.5 μg mL^{-1}. Thus, the proposed sensor can realize not only the rapidly qualitative monitoring of carbaryl by naked eye but also the accurately quantitative assay by spectrophotometry.

The selectivity of AuNCs-MnO_2-AChE − CHO platform for carbaryl detection was studied by testing the interference of other commercial

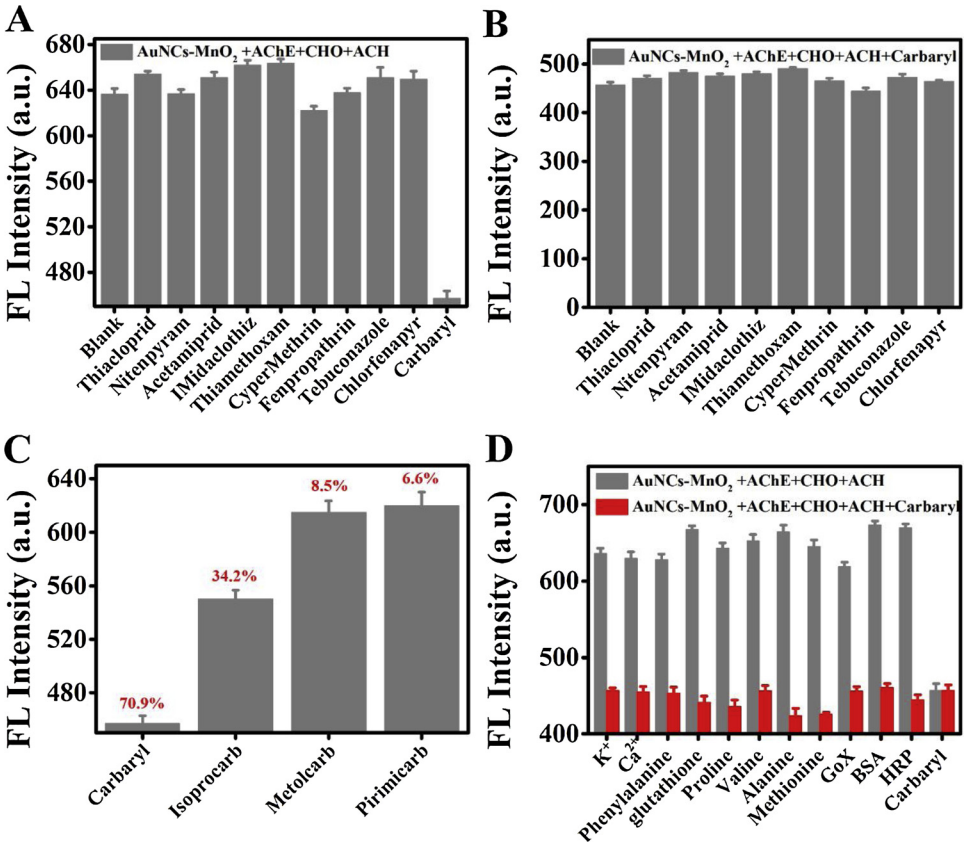

Fig. 5. (A) The selectivity of FL intensity of AuNCs-MnO_2 composite/AChE/CHO system (1000 μg L^{-1} other kinds of pesticides); (B) The anti-influence ability of AuNCs-MnO_2 composite/AChE/CHO system; (C) The FL of 250 μg L^{-1} different carbamate pesticides to AuNCs-MnO_2 composite/AChE/CHO system. (D) The FL intensity of the AuNCs-MnO_2 composite/AChE/CHO system with the interfering substances (1000 μg L^{-1}).

pesticides including neonicotinoid insecticides and pyrethroid pesticides. It can be obviously found that these typical pesticides at the concentration of 1000 μg L^{-1} possess negligible interferences in monitoring of carbaryl (250 μg L^{-1}) (Fig. 5A). What's more, we further investigated the signal response of AuNCs-MnO_2 system to carbaryl in the presence of above pesticides (1000 μg L^{-1}), the sensor still had the same response to carbaryl (Fig. 5B), clearly suggesting that the platform exhibit good selectivity and anti-interference behavior for carbaryl detection. To investigate the response to other carbamate pesticide, three common pesticide including isoprocarb, metolcarb, and pirimicarb were chosen as model analyte. Fig. 5C depicted the FL intensity of system towards carbamate pesticide at the concentration of 250 μg L^{-1}. The IE were 70.9%, 34.2%, 8.5% and 6.6% respectively for carbaryl, isoprocarb, metolcarb and pirimicarb, which may be due to the difference steric hindrance of pesticides, demonstrating that the established assay can be generally utilized for sensing carbamates pesticide. What's more, the performance of the AuNCs-MnO_2-AChE − CHO platform in the presence of common chemical substances was further measured. The influences of some common electrolytes and biological species including K^+, Ca^{2+}, phenylalanine, glutathinione, proline, valine, alanine, methionine, glucose oxidase (GoX), bovine serum albumin (BSA), and horseradish peroxidase (HRP) was investigated in Fig. 5D. After the addition of the above substances (1000 μg L^{-1}), the FL intensity of the AuNCs-MnO_2 system remained nearly constant (FL intensity change less than 5%), while the FL intensity showed obvious quenching signal in the presence of carbaryl (Fig. 5D, red column), indicating that the common electrolytes and biological species also showed negative effect on carbaryl detection. Thus, the AuNCs-MnO_2-AChE − CHO system processed great potential for monitoring carbaryl.

The related strategies for carbaryl detection in the detection limit and detection range was summed up in Table S2. It can be clearly founded that the sensitivity of this strategy was higher than many of the reported assays. Comparing with previous assay, our dual-modality strategy using the AuNCs-MnO_2-AChE − CHO system possessed the following advantages. Firstly, owing to stability of nanocomposite, the specific recognition of enzyme and the pre-processing procedure of samples, such a AuNCs-MnO_2 platform exhibit outstanding anti-interference ability and could offer advantages in accuracy. In previous researches, gold nanoparticle [17] and silver nanoparticle [20] were employed as quencher for the development of carbaryl sensors. The selectivity of these strategies was easily interfered by some common chemicals such as salt, mercapto compounds and cyanide. Moreover, the reduction product Mn^{2+} may be friendly to the environment [40]. Traditional organic fluorophore or quantum dots-based assays displayed relatively high toxicity toward environment. Most importantly, our platform integrates the fluorometric and colorimetric bimodalities into one detection system, from which the monitoring results not only can be preliminarily obtained via naked-eye identification, but also can be accurately detected by fluorescence output with significantly enhanced sensitivity. Thereafter, AuCNs-MnO_2 nanoplatform could be served as a powerful candidate for sensitive detection of carbaryl.

To demonstrate its applicability, the designed platform was further applied for analyzing carbaryl in agricultural and environmental samples (water, soil, rice and apple). For sample pretreatment, carbaryl were extracted by utilizing acetonitrile that cannot dissolve some interference substances (such as GSH, dithiothreitol, H_2O_2 and ascorbic acid). As shown in Fig. 6A, H_2O_2 can obviously influence the detection performance. By taking the pretreatment process (See supporting information), AuNCs-MnO_2-AChE − CHO platform have successfully prevented the effect of H_2O_2, efficiently improving the selectivity for pesticide detection. Then, the present strategy was applied for testing the residues of carbaryl in real samples. As revealed in Table S3, acceptable recoveries between 90.3% and 111.7% with the relative standard deviations (RSDs) lower than 5.06% were collected. Moreover, high-performance liquid chromatography (HPLC), one of the most typically analytical methods of pesticide residues, was also established for carbaryl monitoring. As depict in Fig. 6B, good correlations were obtained between HPLC and the proposed protocol, demonstrating the

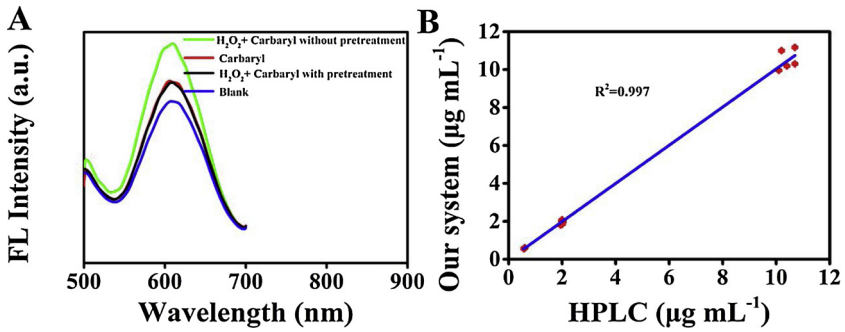

Fig. 6. (A) The fluorescence of AuNCs-MnO_2-AChE − CHO system for pesticide detection. (B) The assay verification of HPLC.

potential applicability of the assay for monitoring carbaryl in practice.

3. Conclusions

In conclusions, we present here a co-template synthesis avenue for AuNCs-MnO_2 nanocomposite. The preparation of nanocomposite not only highly simplified the operation procedure, but also efficiently improving the photostability and chemical stability. Interestingly, by integrating the AChE/CHO-mediated enzymatic reaction, a convenient and sensitive fluorometric/colorimetric bimodal strategy for detecting carbaryl was constructed successfully, processing high sensitivity, acceptable accuracy, and excellent reliability for sensing of real samples. The association of fluorescence output with color recognition, is significant not only for visual detection, but also for mutual authentication in high accuracy manner. Moreover, with no further modification of the nanocomposite, the present platform exhibited many merits including ease-of-use, environmental-friendliness, and cost-effectiveness, indicating that the useful platform could be employed as a promising candidate for the real-time monitoring of carbaryl.

4. Experimental

4.1. Materials

Manganese chloride ($MnCl_2$), hydrogen tetrachloroaurate (III) hydrate ($HAuCl_4{\cdot}xH_2O$), acetylcholinesterase (AChE), choline oxidase (CHO), acetylcholine (ACh) iodide (≥98%), and sodium hydroxide (NaOH) of analytical grade were purchased from Sigma-Aldrich Corporation. Hydrogen peroxide (H_2O_2), phenylalanine (Phe), glutathinione, proline, valine, alanine, methionine, glucose oxidase (GoX), bovine serum albumin (BSA), carbaryl and horseradish peroxidase (HRP) were purchased from Beijing Dingguo Changsheng Biotechnology Co. Ltd (Shanghai, China). The water with good resistivity (> 18 MΩ cm^{-1}) was utilized in this work.

4.2. Preparation of AuCNs-MnO_2 composites

AuNCs-MnO_2 composite were synthesized via a co-template process [38]. Typically, 1.0 mL AuNCs original liquid was mixed with series volume of water. Then, 10–500 μL of $MnCl_2$ solution (50 mmol L^{-1}) were added drop wise into the AuNCs solution, respectively. Thereafter, NaOH solution (1.0 mol L^{-1}) was also added into the solution for mediating pH value to 12 and reacted at strenuous stirring condition for 3 h. The composites were purified rinsing with deionized water for three times. Finally, purified AuCNs-MnO_2 composites were freeze-dried to a brownish black powder. The concentration of AuNCs-MnO_2 nanocomposite was calculated according to Lamber–Beer's Law [34].

4.3. Detection of H_2O_2

Briefly, a serial dilution of H_2O_2 was prepared and stored at 4 °C. Firstly, 100 μL AuNCs-MnO_2 composite were mixed with 100 μL of H_2O_2. The mixture was diluted to 2.0 mL and incubated for 10 min. Then, the FL spectrum were collected under exciting at 370 nm.

4.4. Detection procedure for AChE

50 μL AChE and 50 μL CHO (2 mU mL^{-1}) were mixed with Ach (10 mmol L^{-1}) at 37 °C for incubating 30 min. Then, 100 μL of AuNCs-MnO_2 composite solution were added. After diluted to 2.0 mL, the mixture was incubated for 10 min and tested by FL spectrometer.

4.5. Response of AuNCs-MnO_2 composite to carbaryl

25 μL carbaryl standard solution and 25 μL of AChE were mixed at 37 °C for 20 min. Then, 50 μL ACh and 50 μL CHO were added and incubated at 37 °C for another 30 min. Next, 100 μL of AuNCs-MnO_2 composite was added into the mixture. Finally, the FL spectra were collected.

Competing financial interest

The authors declare no competing financial interest.

Acknowledgements

This work is supported by Science and Technology Development Program of Jilin Province (No. 20170520162JH), the National Key Research and Development Program of China (No. 2016YFC0207300), China Postdoctoral Science Foundation funded project (No. 2018M631862 and 2017M621199) and Postdoctoral Research Foundation funded project by Jilin University (No. 801171090419). X. Yan is thankful for support from the National Postdoctoral Program for Innovative Talents (BX201700096) and the National Nature Science Foundation of China(No. 21806051).

Appendix A. Supplementary data

Supplementary material related to this article can be found, in the online version, at doi:https://doi.org/10.1016/j.snb.2019.04.045.

References

[1] M.G. Lee, V. Patil, Y.C. Na, D.S. Lee, S.H. Lim, G.R. Yi, Highly stable, rapid colorimetric detection of carbaryl pesticides by azo coupling reaction with chemical pre-treatment, Sensor Actuat. B-Chem. 261 (2018) 489–496.
[2] F.C. Moraes, L.H. Mascaro, S.A.S. Machado, C.M.A. Brett, Direct electrochemical determination of carbaryl using a multi-walled carbon nanotube/cobalt phthalocyanine modified electrode, Talanta 79 (2009) 1406–1411.
[3] E. Mauriz, A. Calle, A. Abad, A. Montoya, A. Hildebrandt, D. Barcelo, L.M. Lechuga, Determination of carbaryl in natural water samples by a surface plasmon resonance flow-through immunosensor, Biosens. Bioelectron. 21 (2006) 2129–2136.
[4] Y.H. Song, J.Y. Chen, M. Sun, C.C. Gong, Y. Shen, Y.G. Song, L. Wang, A simple electrochemical biosensor based on AuNPs/MPS/Au electrode sensing layer for monitoring carbamate pesticides in real samples, J. Hazard. Mater. 304 (2016)

103–109.
[5] J. Caetano, S.A.S. Machado, Determination of carbaryl in tomato "in natura" using an amperometric biosensor based on the inhibition of acetylcholinesterase activity, Sensor Actuat. B-Chem. 129 (2008) 40–46.
[6] G. Zimmerman, H. Soreq, Termination and beyond: acetylcholinesterase as a modulator of synaptic transmission, Cell Tissue Res. 326 (2006) 655–669.
[7] I. Cwielag-Piasecka, M. Witwicki, M. Jerzykiewicz, J. Jezierska, Can carbamates undergo radical oxidation in the soil environment? A case study on carbaryl and carbofuran, Environ. Sci. Technol. 51 (2017) 14124–14134.
[8] J.W. Zhou, X.M. Zou, S.H. Song, G.H. Chen, Quantum dots applied to methodology on detection of pesticide and veterinary drug residues, J. Agr. Food Chem. 66 (2018) 1307–1319.
[9] G. Aragay, F. Pino, A. Merkoci, Nanomaterials for sensing and destroying pesticides, Chem. Rev. 112 (2012) 5317–5338.
[10] X. Yan, H.X. Li, W.S. Zheng, X.G. Se, Visual and fluorescent detection of tyrosinase activity by using a dual-emission ratiometric fluorescence probe, Anal. Chem. 87 (2015) 8904–8909.
[11] T.I. Kim, S.B. Maity, J. Bouffard, Y. Kim, Molecular rotors for the detection of chemical warfare agent simulants, Anal. Chem. 88 (2016) 9259–9263.
[12] J.F. Chang, H.Y. Li, T. Hou, F. Li, Paper-based fluorescent sensor for rapid naked-eye detection of acetylcholinesterase activity and organophosphorus pesticides with high sensitivity and selectivity, Biosens. Bioelectron. 86 (2016) 971–977.
[13] X.L. Wu, Y. Song, X. Yan, C.Z. Zhu, Y.Q. Ma, D. Du, Y.H. Lin, Carbon quantum dots as fluorescence resonance energy transfer sensors for organophosphate pesticides determination, Biosens. Bioelectron. 94 (2017) 292–297.
[14] Q. Long, H.T. Li, Y.Y. Zhang, S.Z. Yao, Upconversion nanoparticle-based fluorescence resonance energy transfer assay for organophosphorus pesticides, Biosens. Bioelectron. 68 (2015) 168–174.
[15] Q.S. Mei, H.R. Jing, Y. Li, W. Yisibashaer, J. Chen, B.N. Li, Y. Zhang, Smartphone based visual and quantitative assays on upconversional paper sensor, Biosens. Bioelectron. 75 (2016) 427–432.
[16] X. Yan, H.X. Li, X.G. Su, Review of optical sensors for pesticides, TRAC-Trend Anal. Chem. 103 (2018) 1–20.
[17] D.B. Liu, W.W. Chen, J.H. Wei, X.B. Li, Z. Wang, X.Y.A. Jiang, Highly Sensitive, Dual-Readout Assay Based on Gold Nanoparticles for Organophosphorus and Carbamate Pesticides, Anal. Chem. 84 (2012) 4185–4191.
[18] T. He, L. Qi, J. Zhang, Y.L. Huang, Z.Q. Zhang, Enhanced graphene quantum dot fluorescence nanosensor for highly sensitive acetylcholinesterase assay and inhibitor screening, Sensor Actuat. B-Chem. 215 (2015) 24–29.
[19] L. Lu, H. Su, Q. Liu, F. Li, Development of a Luminescent Dinuclear Ir(III) Complex for Ultrasensitive Determination of Pesticides, Anal. Chem. 90 (2018) 11716–11722, https://doi.org/10.1021/acs.analchem.8b03687.
[20] Z.M. Cui, C.P. Han, H.B. Li, Dual-signal fenamithion probe by combining fluorescence with colorimetry based on Rhodamine B modified silver nanoparticles, Analyst 136 (2011) 1351–1356.
[21] D. Zhao, C.X. Chen, J. Sun, X.R. Yang, Carbon dots-assisted colorimetric and fluorometric dual-mode protocol for acetylcholinesterase activity and inhibitors screening based on the inner filter effect of silver nanoparticles, Analyst 141 (2016) 3280–3288.
[22] N. Li, X.W. Wang, J. Chen, L. Sun, P. Chen, Graphene quantum dots for ultrasensitive detection of acetylcholinesterase and its inhibitors, 2d Mater. 2 (2015) 034018.
[23] Y.D. Zhang, T.T. Hei, Y.A. Cai, Q.Q. Gao, Q. Zhang, Affinity binding-guided fluorescent nanobiosensor for acetylcholinesterase inhibitors via distance modulation between the fluorophore and metallic nanoparticle, Anal. Chem. 84 (2012) 2830–2836.
[24] X. Yan, Y. Song, C.Z. Zhu, H.X. Li, D. Du, X.G. Su, Y.H. Lin, MnO2 nanosheet-carbon dots sensing platform for sensitive detection of organophosphorus pesticides, Anal. Chem. 90 (2018) 2618–2624.
[25] Y.M. Shen, F.M. Yan, X. Huang, X.Y. Zhang, Y.Y. Zhang, C.X. Zhang, J.L. Jin, H.T. Li, S.Z. Yao, A new water-soluble and colorimetric fluorescent probe for highly sensitive detection of organophosphorus pesticides, RSC Adv. 6 (2016) 88096–88103.
[26] X. Gao, G.C. Tang, X.G. Su, Optical detection of organophosphorus compounds based on Mn-doped ZnSe d-dot enzymatic catalytic sensor, Biosens. Bioelectron. 36 (2012) 75–80.
[27] X.W. Meng, J.F. Wei, X.L. Ren, J. Ren, F.Q. Tang, A simple and sensitive fluorescence biosensor for detection of organophosphorus pesticides using H2O2-sensitive quantum dots/bi-enzyme, Biosens. Bioelectron. 47 (2013) 402–407.
[28] Y.H. Yi, G.B. Zhu, C. Liu, Y. Huang, Y.Y. Zhang, H.T. Li, J.N. Zhao, S.Z. Yao, A label-free silicon quantum dots-based photoluminescence sensor for ultrasensitive detection of pesticides, Anal. Chem. 85 (2013) 11464–11470.
[29] H.T. Li, C.H. Sun, R. Vijayaraghavan, F.L. Zhou, X.Y. Zhang, D.R. MacFarlane, Long lifetime photoluminescence in N, S co-doped carbon quantum dots from an ionic liquid and their applications in ultrasensitive detection of pesticides, Carbon 104 (2016) 33–39.
[30] J. Yuan, Y. Cen, X.J. Kong, S. Wu, C.L.W. Liu, R.Q. Yu, X. Chu, MnO_2-Nanosheet-Modified Upconversion Nanosystem for Sensitive Turn-On Fluorescence Detection of H2O2 and Glucose in Blood, ACS Appl. Mater. Inter. 7 (2015) 10548–10555.
[31] R.R. Deng, X.J. Xie, M. Vendrell, Y.T. Chang, X.G. Liu, Intracellular glutathione detection using MnO2-Nanosheet-Modified upconversion nanoparticles, J. Am. Chem. Soc. 133 (2011) 20168–20171.
[32] Q.Y. Cai, J. Li, J. Ge, L. Zhang, Y.L. Hu, Z.H. Li, L.B. Qu, A rapid fluorescence "switch-on" assay for glutathione detection by using carbon dots-MnO_2 nanocomposites, Biosens. Bioelectron. 72 (2015) 31–36.
[33] Y. Xu, X. Chen, R. Chai, C.F. Xing, H.R. Li, X.B. Yin, A magnetic/fluorometric bimodal sensor based on a carbon dots-MnO_2 platform for glutathione detection, Nanoscale 8 (2016) 13414–13421.
[34] W.Y. Zhai, C.X. Wang, P. Yu, Y.X. Wang, L.Q. Mao, Single-layer MnO2 nanosheets suppressed fluorescence of 7-Hydroxycoumarin: mechanistic study and application for sensitive sensing of ascorbic acid in vivo, Anal. Chem. 86 (2014) 12206–12213.
[35] X.L. Zhang, C. Zheng, S.S. Guo, J. Li, H.H. Yang, G.N. Chen, Turn-on fluorescence sensor for intracellular imaging of glutathione using g-C_3N_4 Nanosheet-MnO_2 sandwich nanocomposite, Anal. Chem. 86 (2014) 3426–3434.
[36] Z.Y. Guo, Y.R. Jia, X.X. Song, J. Lu, X.F. Lu, B.Q. Liu, J.J. Han, Y.J. Huang, J.W. Zhang, T. Chen, Giant Gold Nanowire Vesicle-Based Colorimetric and SERS Dual-Mode Immunosensor for Ultrasensitive Detection of Vibrio parahemolyticus, Anal. Chem. 90 (2018) 6124–6130.
[37] W. Zhang, J.Q. Kang, P. Li, H. Wang, B. Tang, Dual signaling molecule sensor for rapid detection of hydrogen sulfide based on modified tetraphenylethylene, Anal. Chem. 87 (2015) 8964–8969.
[38] L. Han, H.J. Zhang, D.Y. Chen, F. Li, Protein-directed metal oxide nanoflakes with tandem enzyme-like characteristics: colorimetric glucose sensing based on one-pot enzyme-free cascade catalysis, Adv. Funct. Mater. 28 (2018) 1800018.
[39] X. Yuan, Z.T. Luo, Q.B. Zhang, X.H. Zhang, Y.G. Zheng, J.Y. Lee, J.P. Xie, Synthesis of highly fluorescent metal (Ag, Au, Pt, and Cu) nanoclusters by electrostatically induced reversible phase transfer, ACS Nano 5 (2011) 8800–8808.
[40] Y.C. Chen, Y.K. Hsu, Y.G. Lin, Y.K. Lin, Y.Y. Horng, L.C. Chen, K.H. Chen, Highly flexible supercapacitors with manganese oxide nanosheet/carbon cloth electrode, Electrochim. Acta 56 (2011) 7124–7130.

Xu Yan received his Ph.D degree from Jilin University under the supervision of Prof. Xingguang Su. He received the Postdoctoral Innovative Talents Supporting Project and then joined Jilin University in 2017 as a postdoctoral. His research interests mainly focus on the development of the functional nanomaterials for chem/bio sensors.

Deshuai Kong is going to get the B. Eng. degree in department of Microelectronics science and engineering, Jilin University in 2018. Now, she is about to assiduously study for her MS degree in College of Electronic Science and Engineering, Jilin University, China. Currently, his research interests mainly focus on the development of the functional nanomaterials for chem/bio sensors.

RuiJin received her M.S. degree in 2016 from College of Chemistry, Jilin University, China. Currently, she is studying for her Ph.D. degree in College of Electronic Science and Engineering, Jilin University. Her research interests mainly focus on the development of the functional nanomaterials for chem/bio sensors.

Xu Zhao received the B.Eng.degree in department of electronic sciences and technology,Jilin University in 2016.Now,he is studying for his MS degree in College of Electronic Science and Engineering,Jilin University,China. Currently, his research interests mainly focus on the development of the functional nanomaterials for chem/bio sensors.

Hongxia Li received her M.S. degree in 2013 from Nanjing Agricultural University. and received her Ph.D. degree in 2016 at Jilin University. Since then, she did postdoctoral work with Prof. Geyu Lu. Currently, her research interests mainly focus on the development of the functional nanomaterials for chem/bio sensors.

Fangmeng Liu received his PhD degree in 2017 from College of Electronic Science and Engineering, Jilin University, China. Now he is a lecturer of Jilin University, China. His current research interests include the application of functional materials and development of solid state electrolyte gas sensor and flexible device.

Yuehe Lin is a professor at Washington State University and a Laboratory Fellow at Pacific Northwest National Laboratory. His research interests include electrochemistry, bioanalytical chemistry, chemical sensors and biosensors, fuel cells and batteries, material synthesis and applications. He has over 10 patents and has published about 400 papers, with total citation ~35,000, H-index 94. He is a fellow of the American Association of the Advancement of Science (AAAS), the Royal Society of Chemistry of the UK, and the American Institute for Medical and Biological Engineering (AIMBE).

Geyu Lu received the B. Sci. degree in electronic sciences in 1985 and the M. Sci. degree in 1988 from Jilin University in China and the Dr. Eng. degree in 1998 from Kyushu University in Japan. Now he is a professor of Jilin University, China. His current research interests include the development of chemical sensors and the application of the function materials.